ATLAS NOTE

ATL-PHYS-PUB-2009-000

March 16, 2009

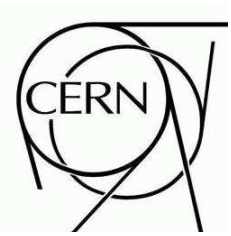

Plans for the Study of the Spin Properties of the Λ_b Baryon Using the Decay Channel $\Lambda_b \to J/\psi(\mu^+\mu^-)\Lambda(p\pi^-)$

The ATLAS Collaboration[1)]

This note is part of CERN-OPEN-2008-020. This version of the note should not be cited: all citations should be to CERN-OPEN-2008-020.

ATL-PHYS-PUB-2009-050
10 May 2009

Abstract

This note summarizes the results of a study of the feasibility of measuring certain spin properties of Λ_b baryon in the ATLAS experiment. We present an assessment of approaches for extracting the inclusive Λ_b polarization and the parity violating α_{Λ_b} parameter for the decay $\Lambda_b \to J/\psi(\mu^+\mu^-)\Lambda(p\pi^-)$ from the reconstructed four final state charged particles. As a key test, we generated Monte Carlo samples of Λ_b events of fixed polarization in the ATLAS detector and evaluated our ability to precisely extract the input polarization from the reconstructed events. The physics motivation for the planned measurements in ATLAS include the search for an explanation of the anomalous spin effects in hyperon inclusive production observed at lower energies, tests of various decay models based on HQET, tests of CP in an area not yet directly explored, and the development of Λ_b polarimetry as a possible tool for spin analysis in future SUSY and other studies.

[1)] This note prepared by M. Biglietti, E. De La Cruz Burelo, H. A. Neal, N. Panikashvili, M. Smizanska and S. Tarem

1 Introduction

We report here plans for the measurement of spin parameters of the Λ_b hyperon. We utilize the decay mode $\Lambda_b \to J/\psi(\mu^+\mu^-)\Lambda(p\pi^-)$ to extract the Λ_b signal from what is expected to be a low background environment, given that the final state has four charged particles and a displaced secondary vertex. The polarization and parity violating α_{Λ_b} parameter will be determined from the relevant angular correlations between the final state particles. We expect to accumulate approximately 13000 Λ_b events (and a similar number of $\overline{\Lambda_b}$) with an integrated luminosity of 30 fb^{-1}. This estimation is based on the latest reconstruction software and trigger simulation for the ATLAS experiment.

The Λ_b is the lightest baryon containing a b quark, and since its discovery in 1991 by the UA1 Collaboration [1] it has created a great deal of interest. Besides the so−called Λ_b lifetime puzzle [2], the Λ_b has been the subject of various theoretical studies ranging from proposed tests of CP violation [3], T violation tests and new physics studies [4], measurement of top quark spin correlation functions [5] and the extraction of the weak phase γ of the CKM matrix [6]. Specific physics interest in the Λ_b parity violating α_{Λ_b} parameter studies derives from its ability to serve as a test for various heavy quark factorization models and perturbative QCD (PQCD). Λ_b studies are also of interest because of the continuing mystery of why hyperons have consistently displayed large polarizations when produced at energies even up to several hundred GeV and at large p_T where most models predict zero polarization. It is not known if these effects can be explained by some not yet understood effect of existing physics or if they point to new physics altogether. Λ_b polarization holds the possibility of illuminating just how polarized b quarks are produced and, indeed, it may have relevance to how fermions are produced in all pp induced processes.

Interest in the studies of the Λ_b lifetime parameter derives from the current controversy from Tevatron experiments concerning the question of how much longer the b quark lives in a meson vs. in a hyperon. With an expected increase of a factor of 100 in the statistics at the LHC, we expect to make a definitive statement on this puzzle. Again, this will further constrain the theoretical models which have as their basis PQCD and the Heavy Quark Model. Lifetime measurements will not be examined in this article, since it is not the focus of the current study, though many of the event selection issues, discussed here, might be applicable in the Λ_b lifetime studies.

We have examined the primary technical challenges in the measurement of Λ_b polarization in ATLAS by generating large samples of Λ_b baryons with various known polarizations, allowing them to decay in the detector using model−predicted amplitudes, and then reconstructing these events using standard ATLAS packages. These samples have permitted us to test our ability to reconstruct events and to confirm that we can recover the input polarization and the decay amplitudes. They also have allowed us to compare various polarization extraction methods and to assess the impact of detector corrections and detector resolution effects. We provide here a report on the results of these studies, and on the work we undertook to adapt the EVTGEN [7] decay package to produce polarized Λ_b within the ATLAS software framework.

2 Theoretical overview

In the quark model the Λ_b is a fermion consisting of a b quark accompanied by a di−quark (ud) of total spin zero. In this model the polarization of the Λ_b is thus expected to be totally due to the b quark polarization. QCD calculations suggest that the b quark polarization would be small. However, there are models of quark scattering [8], in which spin effects are expected to

scale with the mass of the heavy quark, and where the possibility exists for Λ_b polarizations to be quite large. We further note that QCD has not been able to predict the very large polarizations that have been observed in the inclusive production of Λ hyperons at energies of several hundred GeV. It is hoped that the huge mass difference in the b and s quarks will help elucidate the origin of these unexplained spin effects.

Interest in the α_{Λ_b} parameter for the Λ_b stems from the fact that HQET models [9] purport to calculate this quantity from rather basic principles of PQCD and factorization. We have an interest in comparing our ultimate measurements of this quantity with these predictions and assessing what constraints they can provide for these models. We provide below a brief overview of the theoretical basis for the polarization and α_{Λ_b} measurements.

2.1 Heavy quark polarization in QCD

In the Standard Model heavy quark production is dominated by gluon−gluon fusion and $q\bar{q}$ annihilation processes. A non−zero polarization requires an interference between non−flip and spin−flip helicity amplitudes for the Λ_b production, with the latter containing an imaginary part. In QCD this complex part can only be generated through loop corrections, so that the relevant diagrams for polarized quarks are $\mathcal{O}(\alpha_s^4)$. The polarization expected from all QCD sub−processes ($g-g$ fusion, $q\bar{q}$ annihilation and $q-q$, $q-g$ scattering) have been calculated [10]. The formulae for the polarization for each one of the four processes is directly proportional to α_s, and it depends just on the ratio $x_Q = m_Q/p_Q$ and the scattering angle θ_Q, (all defined in the center of mass frame), and are thus valid for any final−state quark Q. The expected polarization in single b quark production by gluon−gluon fusion and $q\bar{q}$ annihilation has been found to be a maximum of 5% for gluon−gluon fusion, and a maximum 10% for $q\bar{q}$ annihilation. When these predictions are compared to the observed Λ polarization (due to the s quark polarization) [11], they are found to be an order of magnitude too small. One might not be surprised if the Λ_b polarization is, as well, greater than predicted in QCD.

An important result in [10] is the dependence of the polarization on the quark mass. The heaviest quark produced is the most polarized, and the maximum polarization is reached around $x_Q \simeq 0.3$. The b quark polarization is predicted to be an order of magnitude greater than the s quark polarization, which from Λ polarization measurements has been found to reach values over 20% at 400 GeV [12].

The measurement of the Λ_b polarization in ATLAS in the exclusive channel $\Lambda_b \to J/\psi\Lambda$ proposed here would cover $p_T(\Lambda_b) > 8000$ MeV (because of trigger and reconstruction constraints on the transverse momentum of the final−state particles, see Table 2) and $x_F(\Lambda_b) < 0.1$. It could make a significant contribution to testing different models of production of polarized baryons in this new kinematic region.

An idea that the heavy quark pre−exists in the incoming proton before scattering and becomes polarized through a direct scattering from an incoming quark provides another pathway for the Λ_b to be polarized. This possibility has been discussed by Neal and Burelo [13]. If polarizations are observed in inclusive Λ_b production that exceed a few percent, such a mechanism should be given careful attention, since no other existing models can account for such large values.

2.2 $\Lambda_b \to J/\psi(\mu^+\mu^-)\Lambda(p\pi^-)$ decay and angular distributions

The proposed study of Λ_b polarization would probe not only the production process but also explore the decay of Λ_b. Decay models predict values for various quantities that can be experimentally observed, thus providing a test of specific HQET/Factorization model [14] assumptions.

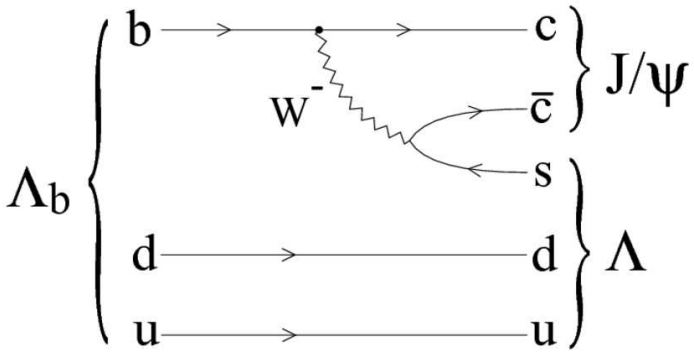

Figure 1: The weak decay of Λ_b: $\Lambda_b \to J/\psi\Lambda$.

The fact that Λ_b has a significant lifetime suggests that it decays weakly. The dominant decay process would involve the emission of a W^- boson, as illustrated in Figure 1. The spin and parity of the particles involved in the $\Lambda_b \to J/\psi(\mu^+\mu^-)\Lambda(p\pi^-)$ decay are well known. The Λ_b with $J^P = \frac{1}{2}^+$ decays to Λ with $J^P = \frac{1}{2}^+$ and J/ψ with $J^P = 1^-$. The general amplitudes for the decay of $\Lambda_b(\frac{1}{2}^+) \to \Lambda(\frac{1}{2}^+)J/\psi(1^-)$ is given by:

$$\mathscr{M} = \overline{\Lambda}(p_\Lambda)\ \epsilon^*_\mu(p_{J/\psi})\ \left[A_1\,\gamma^\mu\gamma^5 + A_2\,\frac{p^\mu_{\Lambda_b}}{m_{\Lambda_b}}\gamma^5 + B_1\,\gamma^\mu + B_2\,\frac{p^\mu_{\Lambda_b}}{m_{\Lambda_b}}\right]\Lambda_b(p_{\Lambda_b}), \tag{1}$$

which is parameterized by the four complex decay amplitudes A_1, A_2, B_1, B_2 and where ϵ_μ is the polarization vector of the J/ψ .

Given the general amplitude, we may compute the helicity amplitudes. We use helicity amplitudes, because they have a direct physical relationship to the spin parameters we wish to study. Four helicity amplitudes are required to describe the decay completely. We will use the notation $H_{\lambda_\Lambda,\lambda_{J/\psi}}$ for the helicity amplitudes of the decay $\Lambda_b \to J/\psi(\mu^+\mu^-)\Lambda(p\pi^-)$, where $\lambda_\Lambda = \pm 1/2$ is the helicity of Λ and $\lambda_{J/\psi} = +1,\ 0,\ -1$ is the helicity of J/ψ . These four helicity amplitudes: $a_+ = H_{1/2,0}$, $a_- = H_{-1/2,0}$, $b_+ = H_{-1/2,1}$, $b_- = H_{1/2,-1}$ are normalized to unity:

$$|a_+|^2 + |a_-|^2 + |b_+|^2 + |b_-|^2 = 1. \tag{2}$$

In this notation, the Λ_b decay asymmetry parameter α_{Λ_b} is given by [15]:

$$\alpha_{\Lambda_b} = \frac{|a_+|^2 - |a_-|^2 + |b_+|^2 - |b_-|^2}{|a_+|^2 + |a_-|^2 + |b_+|^2 + |b_-|^2}. \tag{3}$$

The helicity amplitudes a_+ , a_- , b_+ , b_- are computed directly from the decay amplitudes A_1, A_2, B_1, B_2 according to the following equations:

$$\begin{aligned}
a_+ &= \tfrac{1}{m_{J/\psi}}\left\{\sqrt{Q_+}\left[(m_{\Lambda_b} - m_\Lambda)A_1 - \tfrac{Q_-}{2\,m_{\Lambda_b}}A_2\right] + \sqrt{Q_-}\left[(m_{\Lambda_b} + m_\Lambda)B_1 + \tfrac{Q_+}{2\,m_{\Lambda_b}}B_2\right]\right\},\\
a_- &= \tfrac{1}{m_{J/\psi}}\left\{-\sqrt{Q_+}\left[(m_{\Lambda_b} - m_\Lambda)A_1 - \tfrac{Q_-}{2\,m_{\Lambda_b}}A_2\right] + \sqrt{Q_-}\left[(m_{\Lambda_b} + m_\Lambda)B_1 + \tfrac{Q_+}{2\,m_{\Lambda_b}}B_2\right]\right\},\\
b_+ &= \sqrt{2}\left(\sqrt{Q_+}\,A_1 \mp \sqrt{Q_-}\,B_1\right),\\
b_- &= -\sqrt{2}\left(\sqrt{Q_+}\,A_1 \mp \sqrt{Q_-}\,B_1\right),
\end{aligned} \tag{4}$$

where $Q_{\pm} = (m_{\Lambda_b} \pm m_{\Lambda})^2 - m^2_{J/\psi}$ and m_{Λ_b} and m_{Λ} are the Λ_b and Λ masses respectively [16,17].

The polarization of the Λ_b can be determined from the angular correlations between the $\Lambda_b \to J/\psi\Lambda$ final decay products. The Λ_b polarization reveals itself in the asymmetry of the distribution of the angle θ. This angle is defined as the angle between the normal to the beauty baryon production plane and the momentum vector of the Λ decay daughter, as seen in the Λ_b rest frame. The decay angular distribution can be expressed as:

$$w \sim 1 + \alpha_{\Lambda_b} P \cos(\theta), \tag{5}$$

where α_{Λ_b} is the decay asymmetry parameter of Λ_b and P is the Λ_b polarization [18].

Using the method described in [17], it can be shown that the full decay angular distribution is:

$$w(\vec{\theta}, \vec{A}, P) = \frac{1}{(4\pi)^3} \sum_{i=0}^{i=19} f_{1i}(\vec{A})\ f_{2i}(P, \alpha_\Lambda)\ F_i(\vec{\theta}) \tag{6}$$

where the $f_{1i}(\vec{A})$ are bilinear combinations of the helicity amplitudes and $\vec{A} = (a_+, a_-, b_+, b_-)$. f_{2i} stands for $P\alpha_\Lambda$, P, α_Λ, or 1, where α_Λ is Λ decay asymmetry parameter. F_i are orthogonal angular functions defined in Table 1. The Λ_b decay asymmetry parameter α_{Λ_b} is related to the helicity amplitudes as defined in Equation 3. The five angles $\vec{\theta} = (\theta, \theta_1, \theta_2, \varphi_1, \varphi_2)$ (see Figure 2)

i	f_{1i}	f_{2i}	F_i
0	$a_+a_+^* + a_-a_-^* + b_+b_+^* + b_-b_-^*$	1	1
1	$a_+a_+^* - a_-a_-^* + b_+b_+^* - b_-b_-^*$	P	$\cos\theta$
2	$a_+a_+^* - a_-a_-^* - b_+b_+^* + b_-b_-^*$	α_Λ	$\cos\theta_1$
3	$a_+a_+^* + a_-a_-^* - b_+b_+^* - b_-b_-^*$	$P\,\alpha_\Lambda$	$\cos\theta\ \cos\theta_1$
4	$-a_+a_+^* - a_-a_-^* + \frac{1}{2}b_+b_+^* + \frac{1}{2}b_-b_-^*$	1	$1/2\,(3\cos^2\theta_2 - 1)$
5	$-a_+a_+^* + a_-a_-^* + \frac{1}{2}b_+b_+^* - \frac{1}{2}b_-b_-^*$	P	$1/2\,(3\cos^2\theta_2 - 1)\ \cos\theta$
6	$-a_+a_+^* + a_-a_-^* - \frac{1}{2}b_+b_+^* + \frac{1}{2}b_-b_-^*$	α_Λ	$1/2\,(3\cos^2\theta_2 - 1)\ \cos\theta_1$
7	$-a_+a_+^* - a_-a_-^* - \frac{1}{2}b_+b_+^* - \frac{1}{2}b_-b_-^*$	P, α_Λ	$1/2\,(3\cos^2\theta_2 - 1)\ \cos\theta\cos\theta_1$
8	$-3Re(a_+a_-^*)$	P, α_Λ	$\sin\theta\ \sin\theta_1\ \sin^2\theta_2\ \cos\varphi_1$
9	$3Im(a_+a_-^*)$	$P\,\alpha_\Lambda$	$\sin\theta\ \sin\theta_1\ \sin^2\theta_2\ \sin\varphi_1$
10	$-\frac{3}{2}Re(b_-b_+^*)$	$P\,\alpha_\Lambda$	$\sin\theta\ \sin\theta_1\ \sin^2\theta_2\ \cos(\varphi_1 + 2\,\varphi_2)$
11	$\frac{3}{2}Im(b_-b_+^*)$	$P\,\alpha_\Lambda$	$\sin\theta\ \sin\theta_1\ \sin^2\theta_2\ \sin(\varphi_1 + 2\,\varphi_2)$
12	$-\frac{3}{\sqrt{2}}Re(b_-a_+^* + a_-b_+^*)$	$P\,\alpha_\Lambda$	$\sin\theta\ \cos\theta_1\ \sin\theta_2\ \cos\theta_2\ \cos\varphi_2$
13	$\frac{3}{\sqrt{2}}Im(b_-a_+^* + a_-b_+^*)$	$P\,\alpha_\Lambda$	$\sin\theta\ \cos\theta_1\ \sin\theta_2\ \cos\theta_2\ \sin\varphi_2$
14	$-\frac{3}{\sqrt{2}}Re(b_-a_-^* + a_+b_+^*)$	$P\,\alpha_\Lambda$	$\cos\theta\ \sin\theta_1\ \sin\theta_2\ \cos\theta_2\ \cos(\varphi_1 + \varphi_2)$
15	$\frac{3}{\sqrt{2}}Im(b_-a_-^* + a_+b_+^*)$	$P\,\alpha_\Lambda$	$\cos\theta\ \sin\theta_1\ \sin\theta_2\ \cos\theta_2\ \sin(\varphi_1 + \varphi_2)$
16	$\frac{3}{\sqrt{2}}Re(a_-b_+^* - b_-a_+^*)$	P	$\sin\theta\ \sin\theta_2\ \cos\theta_2\ \cos\varphi_2$
17	$-\frac{3}{\sqrt{2}}Im(a_-b_+^* - b_-a_+^*)$	P	$\sin\theta\ \sin\theta_2\ \cos\theta_2\ \sin\varphi_2$
18	$\frac{3}{\sqrt{2}}Re(b_-a_-^* - a_+b_+^*)$	α_Λ	$\sin\theta_1\ \sin\theta_2\ \cos\theta_2\ \cos(\varphi_1 + \varphi_2)$
19	$-\frac{3}{\sqrt{2}}Im(b_-a_-^* - a_+b_+^*)$	α_Λ	$\sin\theta_1\ \sin\theta_2\ \cos\theta_2\ \sin(\varphi_1 + \varphi_2)$

Table 1: The coefficients f_{1i}, f_{2i} and F_i of the probability density function in Equation 6.

in this probability density function (p.d.f.) have the following meanings:

- θ is the angle between the normal to the production plane and the direction of the Λ in the rest frame of the Λ_b particle;

- θ_1 and ϕ_1 are the polar and azimuthal angles that define the direction of the proton in the Λ rest frame with respect to the direction of the Λ in the Λ_b rest frame;
- θ_2 and ϕ_2, define the direction of μ^+ in the J/ψ rest frame with respect to the direction of the J/ψ in the Λ_b rest frame.

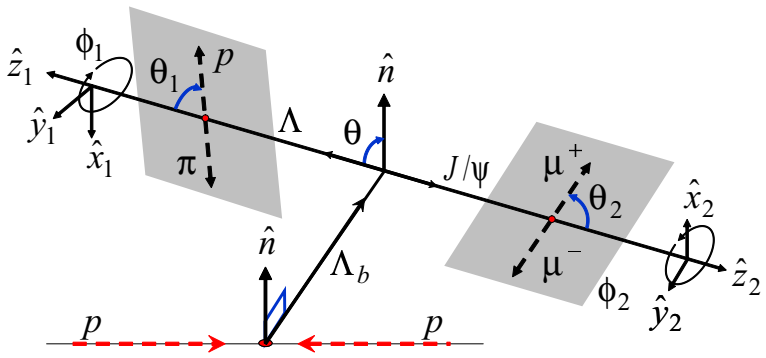

Figure 2: Angles describing the $\Lambda_b \to J/\psi(\mu^+\mu^-)\Lambda(p\pi^-)$ decay.

There are nine unknown parameters in Equation 6. They are the polarization P and four complex helicity amplitudes: $a_+ = |a_+|e^{i\alpha_+}$, $a_- = |a_-|e^{i\alpha_-}$, $b_+ = |b_+|e^{i\beta_+}$, $b_- = |b_-|e^{i\beta_-}$. Using the normalization condition (see Equation 2) and using the fact that the overall global phase is arbitrary, we can reduce the number of unknown independent parameters to seven.

3 Monte Carlo samples

In order to determine if it is feasible to detect polarized Λ_b's in the ATLAS experiment and to measure their polarization, Monte Carlo samples of polarized Λ_b particles were generated using the standard ATLAS software packages. The generation of polarized Λ_b particles and the propagation of their polarization in the decay process required a special treatment, and EVTGEN was adapted for this purpose. The next sections describe how this was implemented in the framework of the ATLAS experiment.

3.1 The generation of polarized Λ_b particles

To generate Λ_b particles, the PYTHIA 6.4 generator [19] is used. Since PYTHIA does not incorporate polarization information from the decay of Λ_b particles, EVTGEN was used to generate the Λ_b decay. EVTGEN provides a general framework for implementation of B hadron decays using spinor algebra and decay amplitudes. This framework permits the proper management of spin correlations of very complicated decay processes. EVTGEN is a Monte Carlo generation package itself, but in this case it is used only to decay the Λ_b particles produced by PYTHIA.

3.1.1 Re−hadronization process and cuts at PYTHIA level

PYTHIA provides mechanisms to produce b quarks, referred to as gluon−gluon fusion, q-$\overline{q}$ annihilation, flavor excitation, and gluon splitting. If all these processes are taken into account, beauty quark events would constitute only 1% of the total number of generated events. In addition, the fraction of b quarks hadronizing to Λ_b is less than 10%. These make the process of Λ_b generation computationally slow. To optimize the generation process, a re−hadronization

step of the same event in the $b\bar{b}$ pairs production is used. In order to avoid repetition of Λ_b events due to the re-hadronization process, a Λ_b pre−selection is implemented at this stage to filter on average only one of the re−hadronized copies of the same event. An additional reason that the Λ_b generation process is slow is that around 95% of final state particles (two muons, a proton, and a pion) of the generated Λ_b events are outside of the η limits ($|\eta| < 2.5$) of the ATLAS detector. In addition, all events must pass the level−1 trigger of the ATLAS trigger system and some pre−reconstruction requirements, such as having a minimum reconstructable transverse momentum. We could not apply these cuts in the PYTHIA step since the kinematics information of the Λ_b children is available only at a later stage, when EVTGEN decays the Λ_b particles. However, by analyzing the p_T and η distributions of Λ_b particles before and after cuts (emulating level−1 and level−2 triggers, and requiring $|\eta| < 2.5$) on the final state particles, we estimated p_T and η limits, below which the Λ_b can not be selected and then applied these cuts in the PYTHIA selection. Figure 3 shows the p_T and η distributions from which the $p_T(\Lambda_b) > 6000$ MeV and $|\eta(\Lambda_b)| < 3$ cuts were selected to filter Λ_b particles in PYTHIA.

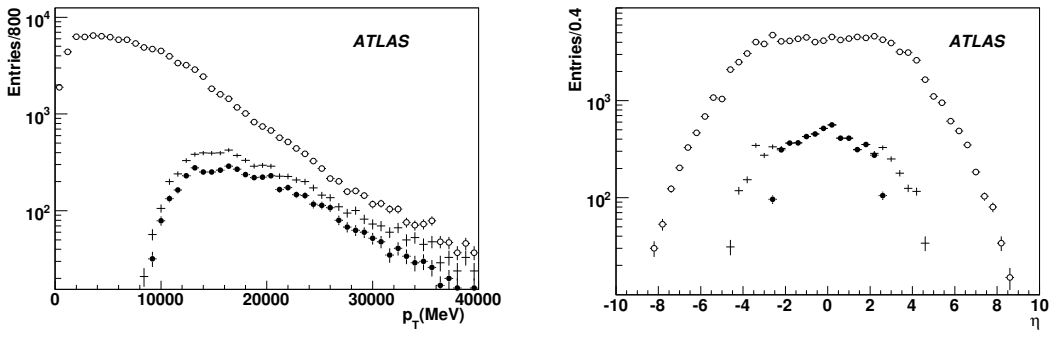

Figure 3: Distributions of p_T (left) and η (right) for Λ_b particles generated using PYTHIA, without cuts (hollow circle), applying η cuts only (cross) and applying all cuts (solid circle) from Table 2.

3.1.2 Setting Λ_b polarization in EVTGEN

To set the polarization of Λ_b particles we used the spin density matrix description of EVTGEN. For the case of spin−1/2 particles like Λ_b the density matrix is defined as:

$$\rho = \frac{1}{2}(I + \vec{P} \cdot \vec{\sigma}) \tag{7}$$

where $\vec{P}$ is the polarization vector, and $\vec{\sigma} = (\sigma_1, \sigma_2, \sigma_3)$, where σ_i is i-th Pauli matrix. In our case $\vec{P}$ is defined as:

$$\vec{P} = P\left(\frac{\hat{z} \times \vec{p}_{lab}(\Lambda_b)}{|\hat{z} \times \vec{p}_{lab}(\Lambda_b)|}\right) \tag{8}$$

where P is the magnitude of the polarization, $\vec{p}_{lab}$ is the momentum of the Λ_b in the laboratory frame, and $\hat{z}$ is the z - axis (along the beam direction) in the ATLAS reference system.

To decay polarized Λ_b we use the HELAMP model of EVTGEN. This model is capable of simulating a generic two body decay with arbitrary spin configuration, taking as input the helicity amplitudes describing the process. In the case of the decay $\Lambda_b \to J/\psi(\mu^+\mu^-)\Lambda(p\pi^-)$, as it has been shown in the previous section, there are four complex helicity amplitudes: a_+, a_-, b_+, and b_-.

The Λ decay into a proton and a pion has been simulated with the same model, using as input parameters the two helicity amplitudes $H_{\lambda_\Lambda,\lambda_p}$ defined in terms of the Λ helicity λ_Λ and the proton λ_p helicity as

$$h_- = H_{-\frac{1}{2},-\frac{1}{2}}, \quad h_+ = H_{+\frac{1}{2},+\frac{1}{2}}. \tag{9}$$

The choice of $h_\pm$ is constrained by the experimentally well known $\Lambda \to p\pi^-$ asymmetry parameter [20]

$$\alpha_\Lambda = |\, h_+ \,|^2 - |\, h_- \,|^2 = 0.642 \pm 0.013. \tag{10}$$

Finally, the decay $J/\psi \to \mu^+\mu^-$ has been described with the EVTGEN VLL (Vector into Lepton Lepton) model [7].

3.1.3 Filtering of $\Lambda_b \to J/\psi(\mu^+\mu^-)\Lambda(p\pi^-)$ events

As a last step in the generation process, we apply kinematic cuts on muons, pion and proton to emulate the fiducial acceptance, level−1 trigger, and pre−reconstruction requirements. These cuts are summarized in Table 2.

Particles	Minimum p_T [MeV]	Maximum $\|\eta\|$
Protons and π's	500	2.7
Most energetic muon	4000	2.7
Other muon	2500	2.7

Table 2: Cuts applied at the particle level.

3.2 Monte Carlo samples and input model for Λ_b decays

As input to the HELAMP class of EVTGEN, the result obtained within the framework of PQCD formalism and the factorization theorem [9] has been used to model the Λ_b decay. From the complex amplitudes calculated in this model, A_1, A_2, B_1, B_2 in Equation 1, the helicity amplitudes a_+ , a_- , b_+ , b_- are calculated by using Equation 4. This is summarized in Table 3. In this model, the Λ_b decay asymmetry parameter, defined in Equation 3, is α_{Λ_b} = -0.457 [2)].

$A_1 = -18.676 - 185.036\,i$	$a_+ = -0.0176 - 0.4229\,i$
$A_2 = -7.461 - 351.242\,i$	$a_- = 0.0867 + 0.2425\,i$
$B_1 = 15.818 - 162.663\,i$	$b_+ = -0.0810 - 0.2837\,i$
$B_2 = -4.252 + 266.653\,i$	$b_- = 0.0296 + 0.8124\,i$

Table 3: PQCD model amplitudes A_i and B_i, are given in units of 10^{-10} and helicity amplitudes $a_\pm$ and $b_\pm$ are normalized to unity.

By using this decay model as input, two Monte Carlo samples were generated with polarizations of -25% and -75%. These Monte Carlo samples were generated, simulated, and fully reconstructed by using the Athena framework [21].

To show how the angular distributions behave, fast Monte Carlo samples (see section 3.3) were generated using an accepted−rejected method based on the p.d.f. defined in Equation 6. Figure 4 shows the distributions of the five angles for helicity amplitudes from Table 3 and polarizations of 40%, 0%, -40%.

[2)] There is an ERRATA in [9] in the reported value of α_{Λ_b} [14].

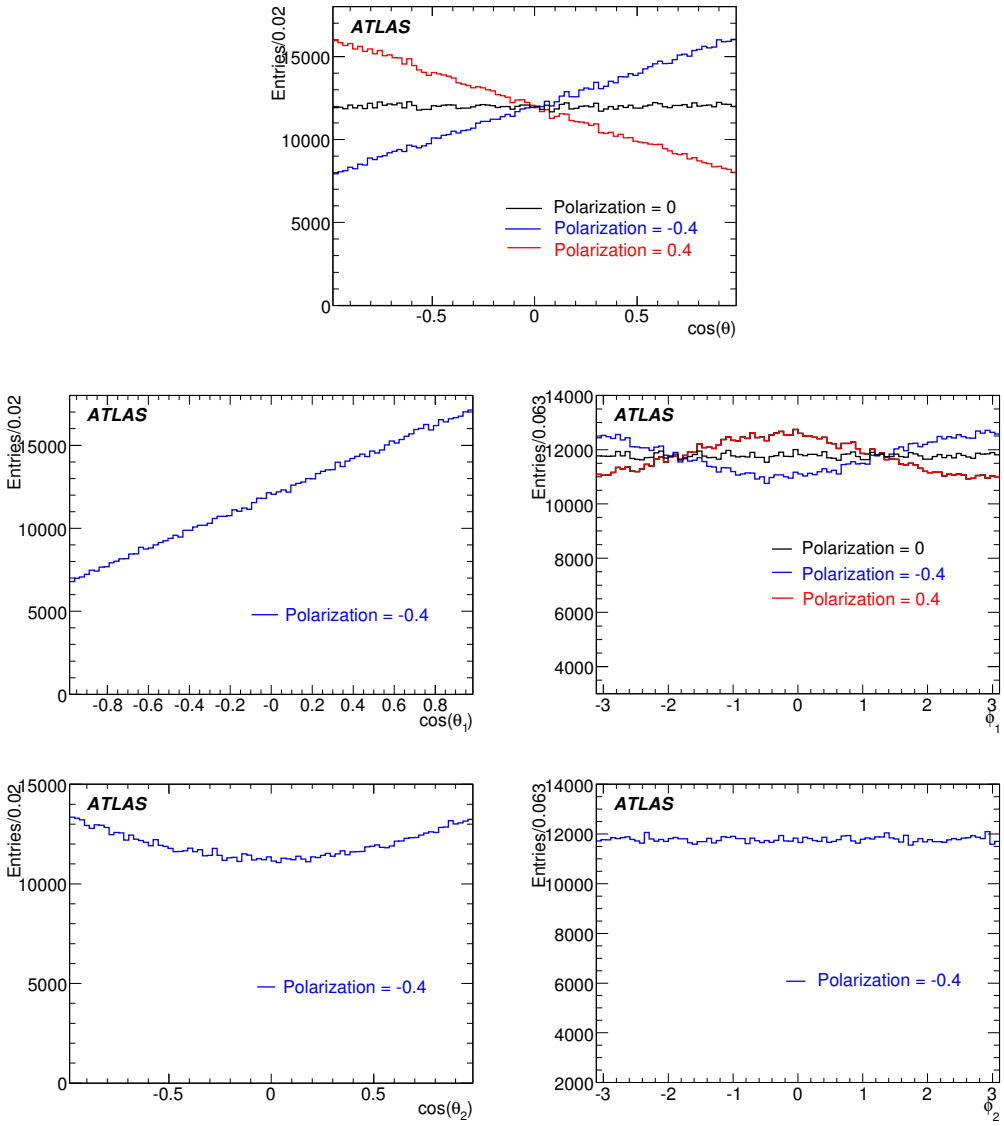

Figure 4: Distributions of the five angles characterizing the decay $\Lambda_b \to J/\psi(\mu^+\mu^-)\Lambda(p\pi^-)$ for different polarization values. For $cos(\theta_1)$, $cos(\theta_2)$, and ϕ_2, all three distributions for the different polarization values look similar, thus only one polarization case is presented.

3.3 Fast Monte Carlo generation

In order to do fast tests of different Λ_b decay models and different polarization values, we need to generate large Monte Carlo samples. This represents a problem due to the computer time required to produce a full chain simulated Monte Carlo data. In order to address this problem a fast Monte Carlo generator was developed. This generator uses Equation 6 to generate angular distributions for the daughters of the Λ_b in the Λ_b rest frame, and then uses a (p, η) distribution derived from phase space of generated events in PYTHIA to compute the kinematic variables of the daughter particles in the laboratory frame. Detector effects are incorporated by using p_T and η cuts on final state particles to mimic di-muon triggers and pre−reconstruction

requirements. Figure 5 illustrates the strong agreement between angular distributions produced by using PYTHIA and EVTGEN Monte Carlo events and fast Monte Carlo events.

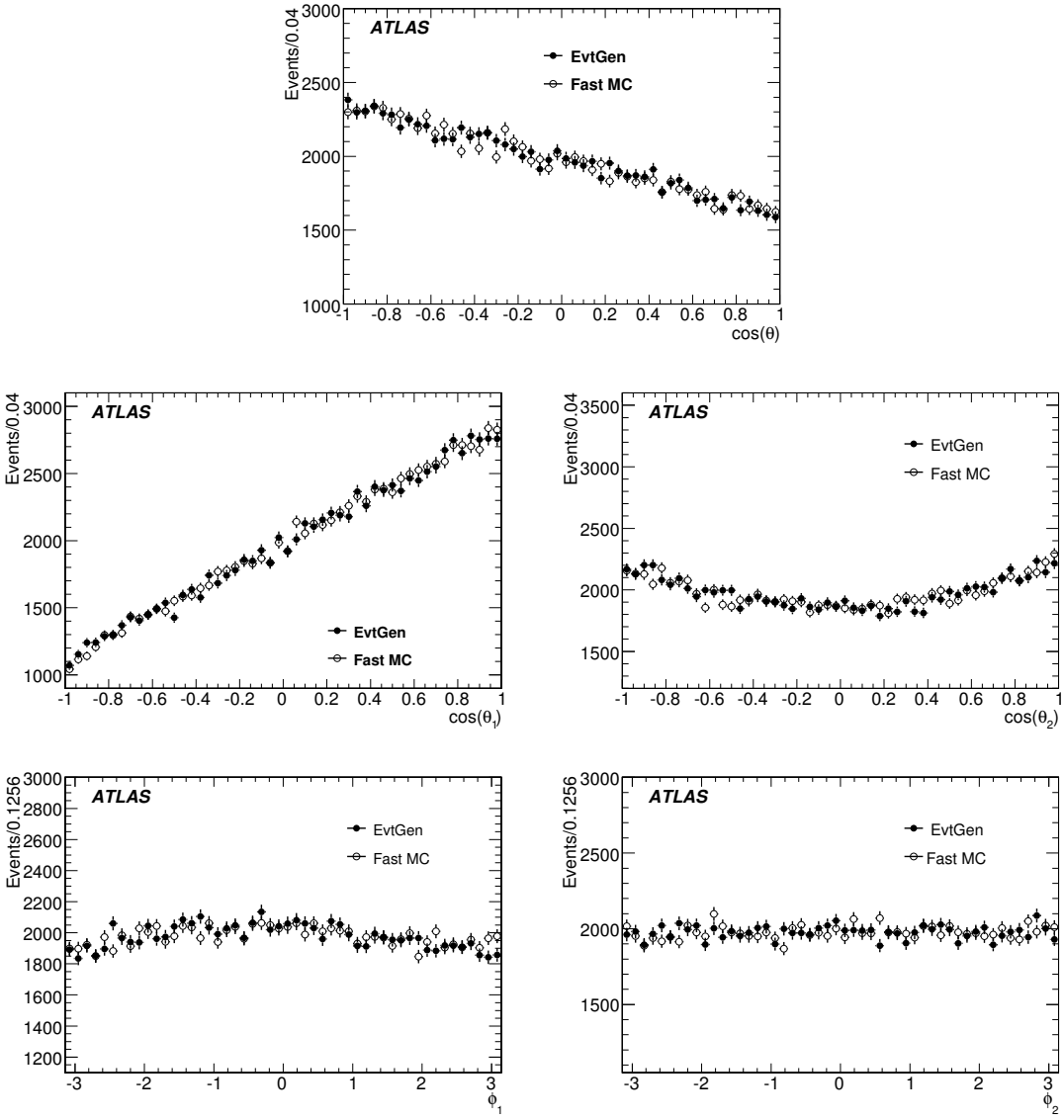

Figure 5: Comparison of Monte Carlo events (PYTHIA + EVTGEN) with fast Monte Carlo generated events. Solid dots represent the Monte Carlo events.

4 Λ_b reconstruction

The reconstruction of Λ_b candidates begins with a search for events with J/ψ candidates. Among these events we search for $\Lambda \to p\pi^-$ candidates, which are then combined with the J/ψ to reconstruct the Λ_b.

4.1 Selection of $J/\psi \to \mu^+\mu^-$ candidates

We search for J/ψ candidates which satisfy the following selection criteria:

- The $\mu^+\mu^-$ candidates must originate at the same reconstructed vertex and the χ^2 of the vertex must be lower than 20;
- The invariant mass of $\mu^+\mu^-$ candidates M($\mu^+\mu^-$) should be within 2800 MeV and 3400 MeV.

The invariant mass distribution of $\mu^+\mu^-$ candidates before applying the invariant mass cuts to select Λ_b is shown in Figure 6.

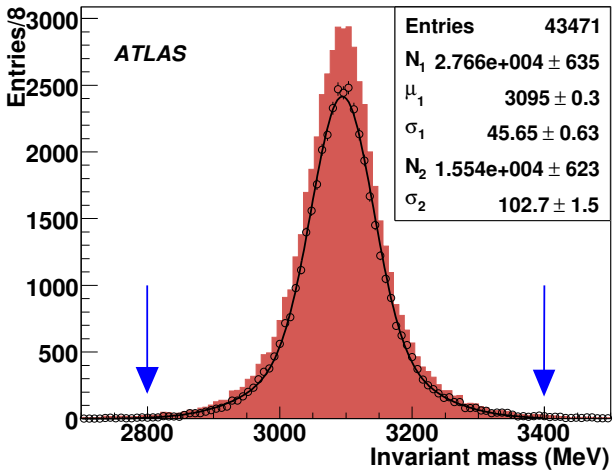

Figure 6: Invariant mass of $\mu^+\mu^-$ candidates. The dark color represents all J/ψ candidates after reconstruction and vertexing requirement. The circles represents J/ψ candidates when level−1 and level−2 trigger signature are required.

4.2 Selection of $\Lambda \to p\pi^-$ candidates

From the previously selected events containing a J/ψ , Λ candidates are selected by applying the following requirements:

- Two opposite charged tracks originating from the same reconstructed vertex.
- The invariant mass of two tracks M($p\pi^-$) should be within 1105 MeV and 1128 MeV range, where for computing M($p\pi^-$), the track with the highest transverse momentum was assumed to be the proton, as observed in 100% of the times in Monte Carlo generations, while the other track was assumed to be a pion.

Many of the Λ particles decay outside of the high−precision part of the Inner Detector, which covers a radius of about 40 cm from the beam line, and thus are lost in reconstruction. The decay vertex position of Λ's in the RZ plane is presented in Figure 8. If the Λ decays outside the 40 cm radius, the number of reconstructed space points (hits in the pixel or silicon layers) is not sufficient for a successful track reconstruction. This effect reduces the fraction of reconstructible Λ to around 60%. Figure 7 presents the invariant mass distribution of the $p\pi^-$ candidates before the invariant mass cuts have been applied.

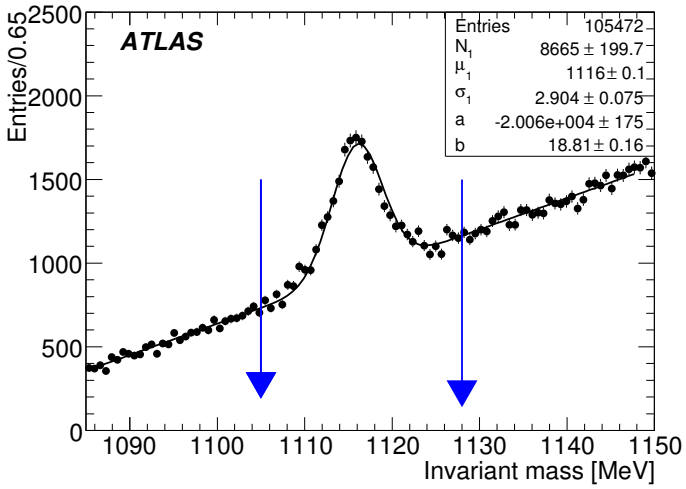

Figure 7: Invariant mass of $p\pi^-$ candidates.

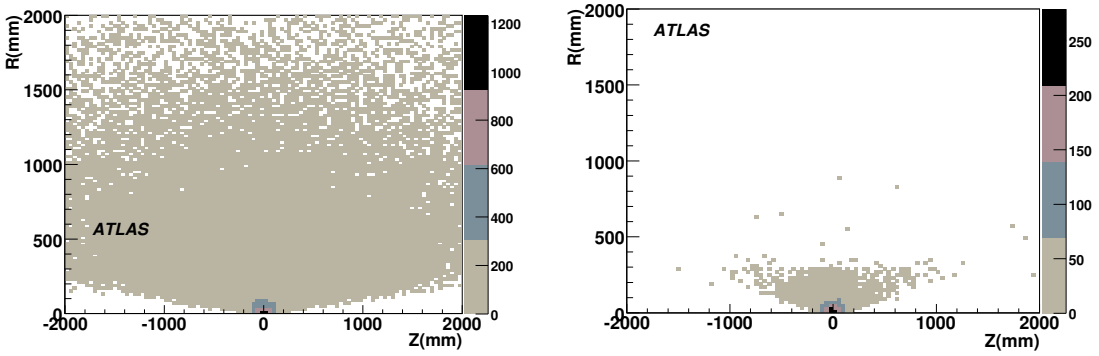

Figure 8: Decay vertex position of Λ's in the RZ plane at the generation level (left) and after reconstruction (right)

.

4.3 Selection of $\Lambda_b \to J/\psi(\mu^+\mu^-)\Lambda(p\pi^-)$ candidates

A previous study [22] based on early ATLAS simulation software estimated that the number of Λ_b and $\overline{\Lambda_b}$ events which we expect to collect for the integrated luminosity of 30 fb^{-1}is 75000. Using the new fully reconstructed sample we made a new estimation. We used the following expression to calculate the number of events:

$$\mathcal{N} = \mathcal{L}\sigma(\Lambda_b)\mathcal{E}, \tag{11}$$

where $\mathcal{L}$ is the integrated luminosity, $\sigma(\Lambda_b) = 7.4$ pb is the cross section of $\Lambda_b \to J/\psi(\mu(p_T > 4000$ MeV$)\mu(p_T > 2500$ MeV$))\Lambda(p(p_T > 500$ MeV$)\pi(p_T > 500$ MeV$))$, see details of the calculation in Table 4, and $\mathcal{E}$ is an overall Λ_b acceptance, which includes the level-1 and level-2 acceptance for $\Lambda_b \to J/\psi(\mu^+\mu^-)\Lambda(p\pi^-)$.

For selecting events with b hadrons at a luminosity below about $10^{33}cm^{-2}s^{-1}$, the first level trigger will require the presence of a muon with p_T $>$ 6000 MeV within the trigger geometric

$\sigma(pp \to \Lambda_b X)$	0.00828113 mb
BR ($\Lambda_b \to J/\psi\Lambda$)	$(4.7 \pm 2.8) \times 10^{-4}$ [20]
BR ($\Lambda \to p\pi^-$)	$(63.9 \pm 0.5) \times 10^{-2}$ [20]
BR ($J/\psi \to \mu^+\mu^-$)	$(5.93 \pm 0.06) \times 10^{-2}$ [20]
Including cuts	0.05
Overall cross-section	**7.4 pb**

Table 4: The cross-section calculation of $\Lambda_b \to J/\psi(\mu^+\mu^-)\Lambda(p\pi^-)$ decay.

acceptance of $|\eta| < 2.4$. The effect of the level−1 trigger threshold on muon p_T is not a sharp cut and a fraction of muons with p_T lower than 6000 MeV will be collected. Figure 9 shows the efficiency of the level−1 simulation with nominal p_T threshold of 6000 MeV as function of p_T . Around 69% of events with $J/\psi \to \mu^+\mu^-$, where one muon has p_T > 4000 MeV and the second muon has p_T > 2500 MeV, passed the level−1 trigger simulation. Therefore a signal dataset with p_T less than 6000 MeV has been chosen to study all possible triggered events with low p_T muons instead of a usual sharp 6000 MeV cut.

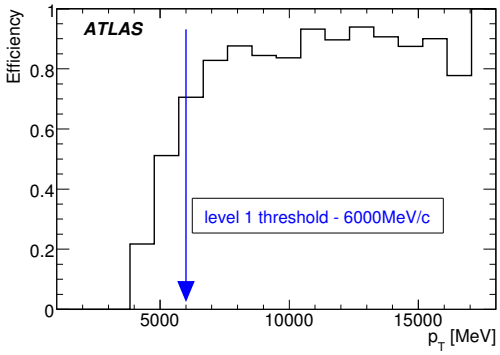

Figure 9: The level−1 trigger simulation efficiency as a function of muon p_T , obtained from the Λ_b signal sample over the whole detector volume.

Further selections in the high level trigger are based on the Region of Interest (RoI) identified at level−1, as follows: a search for a second muon close to the trigger muon is used to select channels containing two final state muons, for example from J/ψ . It is based on expanding the level−1 muon RoI to find a second muon which was not triggered by level−1. This increases the efficiency of the di−muon trigger by extending the p_T acceptance for the second muon down below 6000 MeV. The size of the increased RoI is based on the distribution of angular distance in η and ϕ between two muons decayed from J/ψ . The Inner Detector tracks which are reconstructed within these RoI, are then extrapolated to the muon system to find the corresponding hits within the window. The Inner Detector tracks associated with the muon spectrometer hits can be identified as muons. The level−2 trigger efficiency is found to be around 78% for $\Lambda_b \to J/\psi(\mu(p_T > 4000 \text{ MeV})\mu(p_T > 2500 \text{ MeV}))\Lambda(p(p_T > 500 \text{ MeV})\pi(p_T > 500 \text{ MeV}))$.

We reconstruct the Λ_b by performing a constrained fit to a common vertex for the two muon tracks and Λ , with the two muon tracks constrained to the J/ψ mass of 3097 MeV [20]. The reconstruction efficiency depends on the cuts which will be applied on all Inner Detector tracks in the reconstruction stage to reduce the fake rate. The overall efficiency is found to be

around 6.1% if the p_T threshold is 500 MeV, see Table 5. Figure 10 shows the invariant mass distribution of Λ_b candidates. Simulation of the level−1 trigger with level−1 p_T thresholds of 6000 MeV and 4000 MeV and level−2 trigger, explained above, included in the analysis. We expect to collect around 13500 (13100) $\Lambda_b \to J/\psi(\mu^+\mu^-)\Lambda(p\pi^-)$ events using 4000 MeV (6000 MeV) level−1 muon threshold for the integrated luminosity of about 30 fb^{-1}.

level−1 trigger:	one muon		two muons	
with p_T threshold	4 GeV	6 GeV	4GeV	6GeV
level−2 trigger:	TrigDiMuon		Topological trigger	
J/ψ reconstruction efficiency including level-1 and level-2 triggers	42%	39%	27.5%	10%
Λ reconstruction efficiency	15%			
Λ_b overall efficiency	6.1%	5.9%	5.4%	3.5%

Table 5: The overall Λ_b efficiency depending on the trigger strategy.

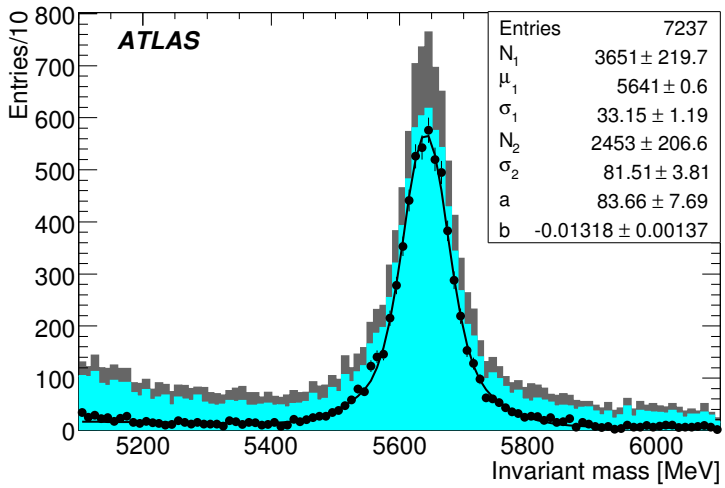

Figure 10: $\mu^+\mu^-$ Λ invariant mass distribution. The dark color represents all Λ_b candidates after reconstruction and vertexing requirement, and the light color represents the case when a level−1 and level−2 trigger signature is required in addition. Filled circles represents data after all selection cuts. The fit is the result of using double Gaussian and Polynomial functions.

We need to acknowledge that there are other inefficiencies that will appear when we analyze the real data. For example, even if the individual track reconstruction efficiency is as high as 98%, we will have an overall reduction in event rate of about 10%. Even if such reductions occur, we still expect the final sample to be sufficient for a meaningful measurement of the Λ_b polarization.

4.4 Angular distributions and angular resolutions

The reconstruction efficiency modifies the angular distributions used in the polarization determination. Figure 11 shows how the angular distributions change due to detector acceptance for a Monte Carlo sample with polarization of -75%.

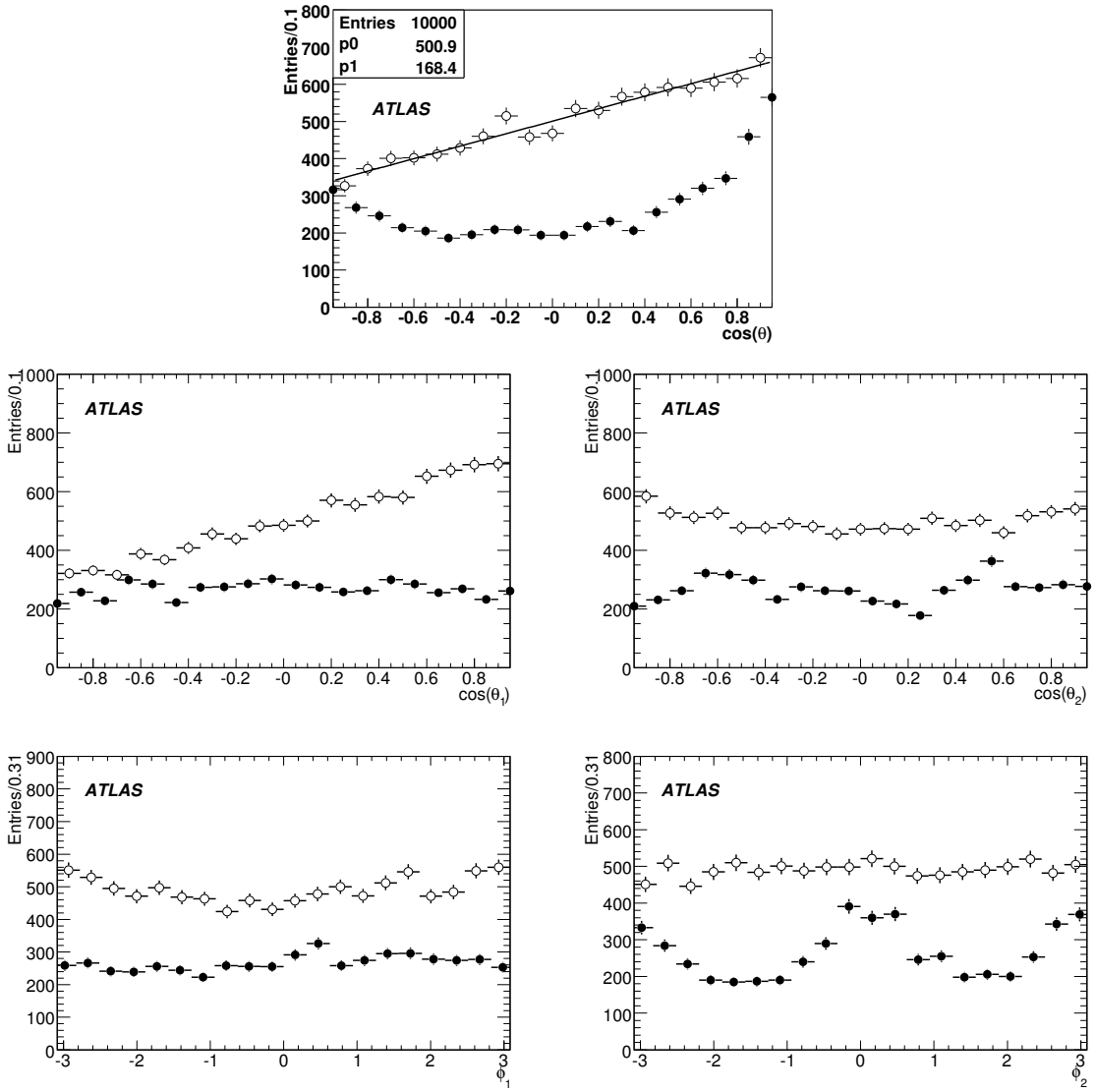

Figure 11: Comparison of fast Monte Carlo events without kinematics and detector acceptance cuts (open circles) and Monte Carlo events after full detector simulation and reconstruction (solid circles).

The angular resolution of the five angles is presented in Figure 12. We used this angular resolution in the statistical uncertainty study.

4.5 Background

Due to its production rate the main background source for our Λ_b reconstruction will be the prompt production and decay of $J/\psi \to \mu^+\mu^-$ which are then combined with Λ candidates in the event. However, the long lifetime of the Λ_b allows us to reduce significantly this kind of background by applying a lifetime cut. After a Λ_b lifetime cut (a cut of 200 μm on the proper transverse decay length), this background was found to be negligible and it is not considered in

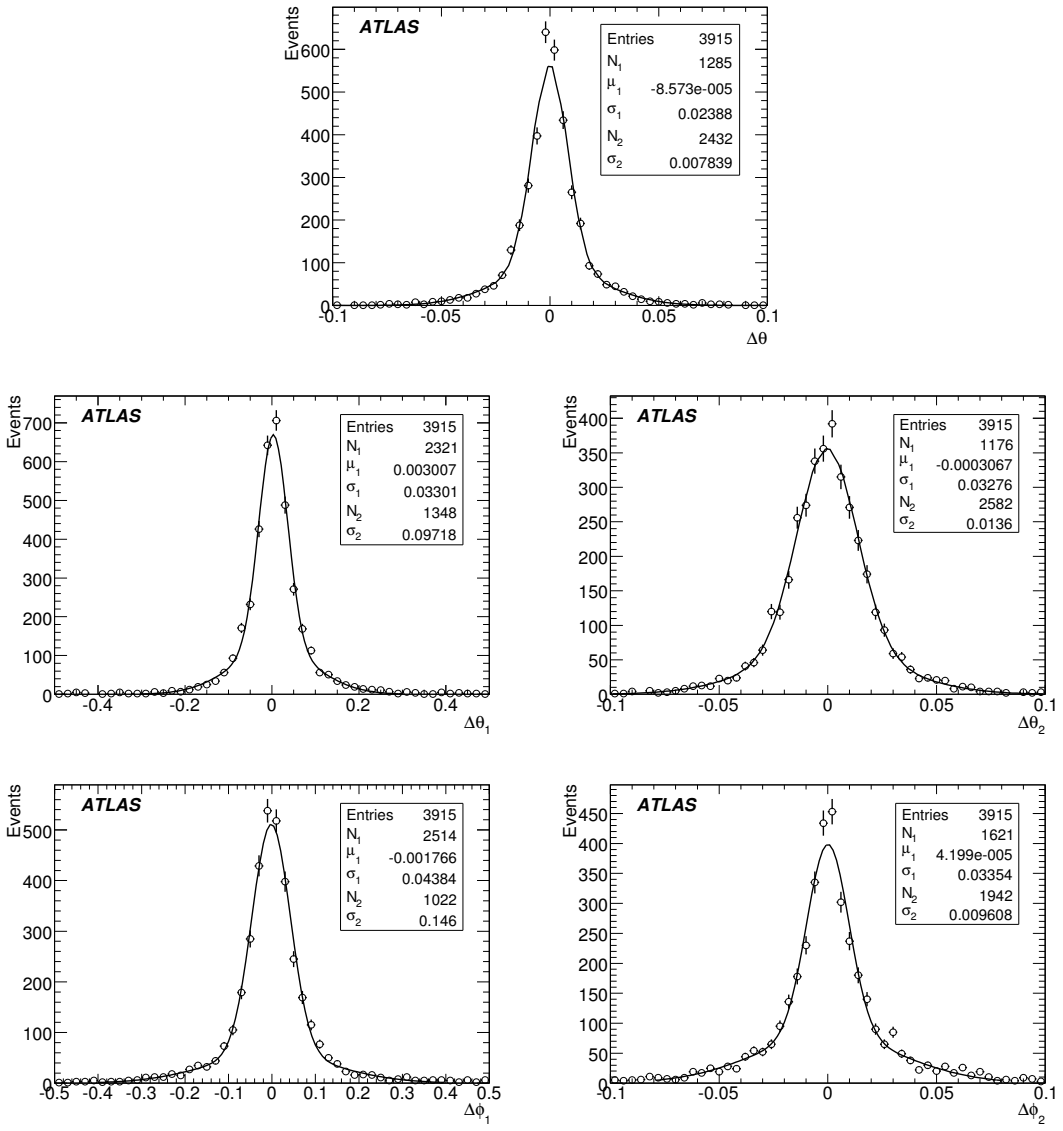

Figure 12: Angular resolution from fully simulated Monte Carlo data. The fit is the result of using double Gaussian distributions.

this study.

In order to investigate the different contributions of long−lived background particles not removed by the lifetime cut mentioned above, we used a inclusive J/ψ Monte Carlo sample of $b\bar{b} \to J/\psi X$ requiring in addition to a J/ψ , a Λ in each event ($b\bar{b} \to J/\psi \Lambda X$). This Λ could be produced along with the J/ψ from a B hadron decay or just be part of the event, and the invariant mass of the $J/\psi + \Lambda$ combination should be within 5100 - 6100 MeV. Figure 13 shows the invariant mass distributions of Λ_b candidates reconstructed in this Monte Carlo sample. The observed level of background under the Λ_b signal is of few percents, and it is considerably reduced after extra cuts like the lifetime cut mentioned above. In Figure 13 another wider distribution due to $\Lambda_b \to J/\psi \Sigma^0(\Lambda\gamma)$ is observed very close to our $\Lambda_b \to J/\psi \Lambda$ signal. This is due to the branching ratios of both decays channels being the same as set by default in PYTHIA. This

behavior has not been observed at Tevatron experiments where hundreds of $\Lambda_b \to J/\psi\Lambda$ events are reconstructed. Therefore we expect the branching ratio of the $\Lambda_b \to J/\psi\Sigma^0(\Lambda\gamma)$ decay to be considerably smaller than the branching ratio of the $\Lambda_b \to J/\psi\Lambda$, and that the resulting background will be much smaller than shown.

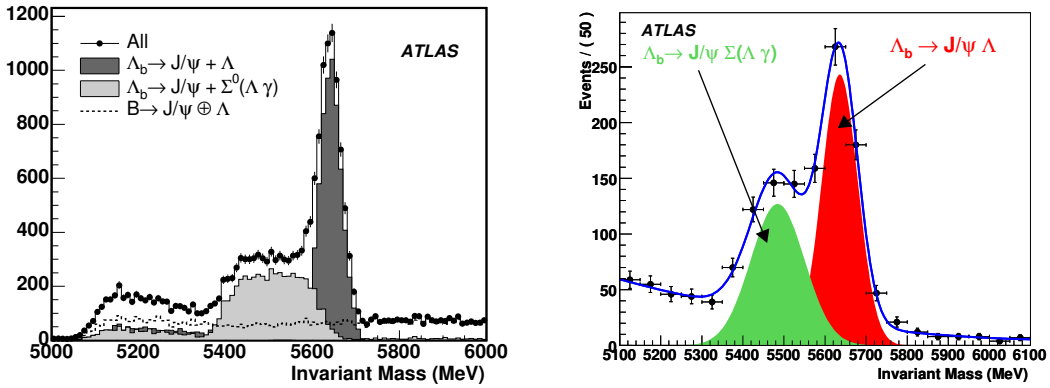

Figure 13: Invariant mass distribution from Λ_b candidates identified in $b \to J/\psi\Lambda X$ Monte Carlo sample. Composition at generation level with smearing from reconstruction (left) and fit to the fully reconstructed events (right) after vertexing requirement are shown.

5 Extracting Λ_b polarization and decay parameters

5.1 Fitting method

5.1.1 Likelihood function

To extract polarization and decay amplitudes we performed an un−binned maximum likelihood fit to the angular distributions. The log−likelihood function $\mathcal{L}$ is defined by:

$$\mathcal{L} = -2\sum_{j=1}^{N} \log(w_{obs}(\vec{\theta'}, \vec{A}, P)), \tag{12}$$

where

$$w_{obs}(\vec{\theta'}, \vec{A}, P) = \frac{\int w(\vec{\theta'}, \vec{A}, P)T(\vec{\theta}, \vec{\theta'})d\vec{\theta}}{\int\int w(\vec{\theta'}, \vec{A}, P)T(\vec{\theta}, \vec{\theta'})d\vec{\theta}d\vec{\theta'}}. \tag{13}$$

$w(\vec{\theta'}, \vec{A}, P)$ is the p.d.f defined in Equation 6, $\vec{\theta'}$ are the measured angles, $\vec{\theta}$ are angles without detector effects, and $T(\vec{\theta}, \vec{\theta'})$ is defined as

$$T(\vec{\theta}, \vec{\theta'}) = \epsilon(\vec{\theta})R(\vec{\theta}, \vec{\theta'}), \tag{14}$$

where $\epsilon(\vec{\theta})$ is the efficiency function and $R(\vec{\theta}, \vec{\theta'})$ is the resolution function.

In the ideal case the resolution function is:

$$R(\vec{\theta}, \vec{\theta'}) = \delta(\vec{\theta} - \vec{\theta'}), \tag{15}$$

then we have

$$w_{obs}(\vec{\theta'}, \vec{A}, P) = \frac{w(\vec{\theta'}, \vec{A}, P)\epsilon(\vec{\theta'})}{\sum_{i=0}^{i=19} f_{1i}(\vec{A}) f_{2i}(P\alpha_\Lambda)\mathcal{F}_i}, \tag{16}$$

where $\mathcal{F}_i = \int F_i(\vec{\theta})\epsilon(\vec{\theta})d\vec{\theta}$ are the acceptance corrections values, which have to be calculated in advance to perform the fit.

The final log−likelihood may be re−written as a sum of two terms:

$$L = -2\sum_{j=1}^{N}[\log(\frac{w(\vec{\theta'}, \vec{A}, P)}{\sum_{i=0}^{i=19} f_{1i}(\vec{A}) f_{2i}(P\alpha_\Lambda)\mathcal{F}_i}) + \log(\epsilon(\vec{\theta'}))]. \tag{17}$$

Since the second term does not depend on the parameters we want to measure, the main challenge is to find the acceptance function.

5.1.2 Detector acceptance corrections

The acceptance corrections integral $\mathcal{F}_i = \int F_i(\vec{\theta})\epsilon(\vec{\theta})d\vec{\theta}$ can be approximated by the following form, using the Monte Carlo integration techniques

$$\mathcal{F}_i \approx \frac{1}{N_{gen}} \sum_{j=0}^{j=N_{acc}} \frac{F_i(\vec{\theta})}{G(\vec{\theta})}, \tag{18}$$

where N_{gen} is the number of generated events, N_{acc} is the number of accepted events after the simulation of the fiducial acceptance and p_T cut and G is the p.d.f which has been used to generate the θ.

If the generation of the events is done using certain p.d.f (w), the acceptance can be calculated by the simple expression:

$$\mathcal{F}_i \approx \frac{1}{N_{gen}} \sum_{j=0}^{j=N_{acc}} \frac{F_i(\vec{\theta})}{w(\vec{\theta}, \vec{A}, P)}. \tag{19}$$

We used this expression to calculate the acceptance in the case when w is the p.d.f from Equation 6.

This method can be used under the assumption that the acceptance does not depend on the measured parameters, and that the angular resolutions are close enough to the ideal resolutions. In order to check the first assumption we plotted the ratio

$$\frac{\int w(\vec{\theta}, \vec{A}, P)\epsilon(\vec{\theta}, \vec{A}, P)d\vec{\theta}}{\int w(\vec{\theta}, \vec{A}, P)\epsilon(\vec{\theta}, \vec{A}, P=0)d\vec{\theta}} \tag{20}$$

for the different polarization values (see Figure 14). No significant dependence of the acceptance on the polarization is observed in this test.

The angular resolutions are shown in Figure 12. To test the effect of these resolutions, Monte Carlo fits were performed including a smearing of the data based on the Gaussian fits in Figure 12. Fit results with and without smearing are consistent within the statistical uncertainty. Figure 15 shows, as an example, a comparison of fit results for a sample of 2000 events with polarization of -75% when fits are performed on the sample of generated Monte Carlo events.

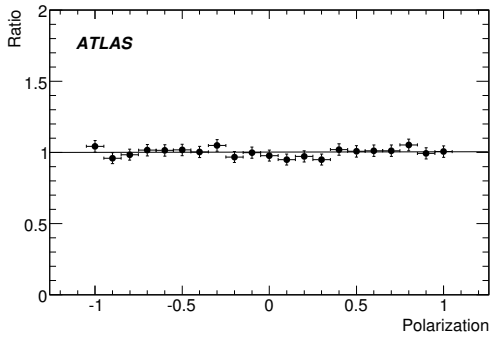

Figure 14: Ratio defined in Equation 20 as a function of polarization.

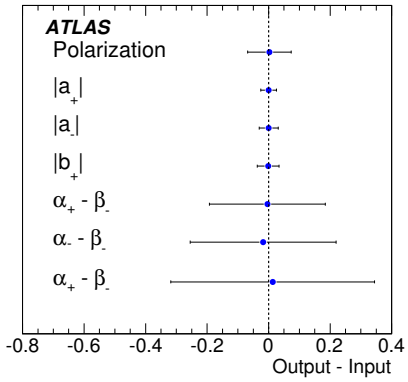

Figure 15: Comparison of fit outputs from generation level Monte Carlo with and without Gaussian smearing due to finite angular resolution. Error bars are statistical uncertainties from the fit with Gaussian smearing included.

5.2 Fits to fully simulated Monte Carlo data

In order to extract polarization and decay parameters from the Monte Carlo data samples, final Λ_b selection cuts were applied. A proper transverse decay length greater than 200 μm is required to remove contamination from prompt produced J/ψ events. The proper transverse decay length for the Λ_b candidate is given by:

$$\lambda = \frac{L_{xy}}{(\beta\gamma)_T^{\Lambda_b}} = L_{xy}\frac{cM_{\Lambda_b}}{p_T}, \tag{21}$$

where $(\beta\gamma)_T^{\Lambda_b}$ and M_{Λ_b} are the transverse boost and the mass of the Λ_b, and L_{xy} is a transverse decay length. The transverse decay length is defined as $L_{xy} = \boldsymbol{L}_{xy} \cdot \boldsymbol{p}_T/p_T$ where $\boldsymbol{L}_{xy}$ is the vector that points from the primary vertex to the Λ_b decay vertex and $\boldsymbol{p}_T$ is the transverse momentum vector of the Λ_b. A minimum p_T of 500 MeV is required for any track used in the Λ_b reconstruction. In addition, a $p_T > 4000$ MeV is required for the muon with larger p_T, and $p_T > 2500$ MeV for the second muon. These cuts reduce the Λ_b sample by 21%, mainly due to the lifetime cut.

Table 6 shows the results of performing a likelihood fit to our fully simulated Monte Carlo

Parameter	Value ± Uncertainty (Polarization = -25%)	Value ± Uncertainty (Polarization = -75%)	Value (Input at generation level)
Polarization	-0.213 ± 0.069	-0.882 ± 0.064	-0.25/-0.75
$\|a_+\|$	0.461 ± 0.051	0.413 ± 0.023	0.429
$\|a_-\|$	0.289 ± 0.058	0.161 ± 0.035	0.260
$\|b_+\|$	0.259 ± 0.071	0.370 ± 0.027	0.295
$\alpha_+ - \beta_-$	-0.991 ± 0.640	-2.050 ± 0.134	-1.612
$\alpha_- - \beta_-$	0.856 ± 0.364	0.681 ± 0.342	1.231
$\beta_+ - \beta_-$	-1.442 ± 0.666	-2.624 ± 0.187	-1.849

Table 6: Fit results from fully simulated and reconstructed Monte Carlo events with input polarization of -25% and -75%.

data, for a sample of 2000 Λ_b events, corresponding to around 5 fb^{-1}of collected data. Figure 16 shows the difference between the input values in Monte Carlo and the extracted values of polarization and decay parameters by the likelihood fit. We used as fitting parameters: $|a_+|$, $|a_-|$, $|b_+|$, $\alpha_+ - \beta_-$, $\alpha_- - \beta_-$, $\beta_+ - \beta_-$, and the polarization P.

Detector acceptance corrections in Equation 19 were computed separately from the two Monte Carlo samples with different polarizations which are used in this study. Corrections computed in the Monte Carlo sample of -75% polarization were used in the fit of the Monte Carlo sample of -25% polarization, and vice versa. Due to the limited statistics in the Monte Carlo samples used to calculate the acceptance corrections defined in Equation 19, a bagging (from bootstrap aggregating) technique [23] was used to generate multiple samples in order to avoid the effect of statistical fluctuations. This technique consists of generating replicates of a data set by selecting at random events from the original data set allowing repetition of events. We generated 1000 bootstrap replicates of the fully simulated Monte Carlo data sample. The $\mathcal{F}_i$ factors (Equation 19) were computed from each generated data sample and the average was taken as the value for each of the twenty $\mathcal{F}_i$ correction factors. Systematic uncertainty due to the width of the correction factors distributions in these 1000 generated data sets was estimated by repeating the fit to fully simulated Monte Carlo using the $\mathcal{F}_i$ values from the each of the generated samples, and assigning the width of the distribution of fitted parameters as a systematic uncertainty. This systematic error (also shown in Figure 16) can be reduced with more Monte Carlo statistics for the $\mathcal{F}_i$ calculation.

5.3 Estimate of statistical uncertainties

To estimate statistical uncertainties as a function of polarization, we used a fast Monte Carlo probabilistic approach to generate polarized Λ_b particles. The fast Monte Carlo includes angular resolution from the fully reconstructed samples and detector acceptance simulation. We generated a large number of samples with different values of polarization. A maximum likelihood fit was used to extract the decay parameters and the polarization. Detector acceptance corrections were calculated from high statistics fast Monte Carlo data simulated without polarization. Figure 17 presents the expected statistical uncertainty in the polarization P and in α_{Λ_b} as a function of the polarization value for the integrated luminosity of 30 fb^{-1}. The study was done for α_{Λ_b} = -0.457 with the same input model as used in fully simulated Monte Carlo. In Figure 17 also the correlation between α_{Λ_b} and P is shown as a function of polarization. The correlation values were extracted from the Maximum Likelihood fit results.

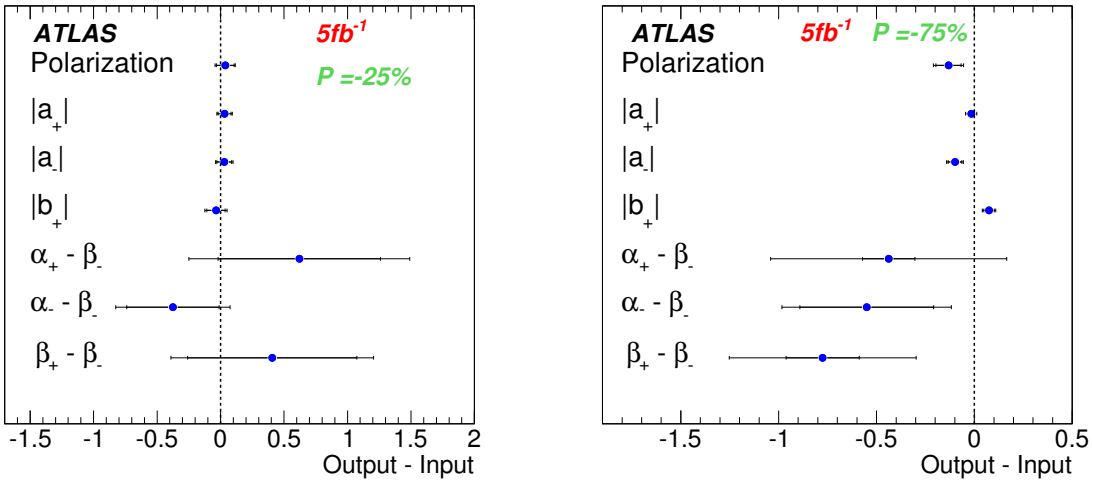

Figure 16: Comparison of fit results for polarization of -25% (left) and -75% (right) with respect to input values from Monte Carlo generation. The statistical and systematic uncertainties are included.

In our study we used specific set of decay amplitudes, presented in Table 3, to demonstrate our ability to extract these parameters. To insure that the success of our analysis techniques did not depend on the amplitudes chosen, we conducted a fast Monte Carlo study using a different model with $\alpha_{\Lambda_b} = 0.1$ [24] to test our procedure in a case of smaller α_{Λ_b} value. We found that it is possible to satisfactorily extract α_{Λ_b} and the polarization even with such a change in the amplitude values.

6 Results and conclusions

In this note we have presented the results from a series of studies to determine if polarized Λ_b baryons can be reconstructed in ATLAS and have their polarization and α_{Λ_b} parameter measured. Our results indicate that the answer is affirmative. Λ_b events should be identifiable through the reconstruction of their four charged final state particles, and the angles between these particles can be measured with sufficient accuracy to determine the parent's polarization. With trigger constraints and detector cuts fully specified, our more complete analysis suggests that the number of events we should expect after 30 fb^{-1}of data will only be 13,000, compared to the 37,500 noted in the ATLAS-TDR [22]. Different additional detector and background effects, which are difficult to model at the current level of detector description, can further reduce the signal sensitivity. These effects could include the detector and trigger inefficiency, misalignment, pile-up events and increased combinatorial background due to e.g. the fake tracks. Nevertheless, even with a reduction of 50%, a polarization measurement with a statistical uncertainty of several percent should be possible in a regime where polarization is larger than 25% as experimentally measured at lower energies. Efforts will continue to develop algorithms to improve the various reconstruction and trigger efficiencies and in consequence providing an enhanced yield of reconstructed particles in data samples.

We note that almost all models predict that the Λ_b polarization at the LHC at small Feynman x should be vanishingly small. Measurement of a significant polarization would have to be

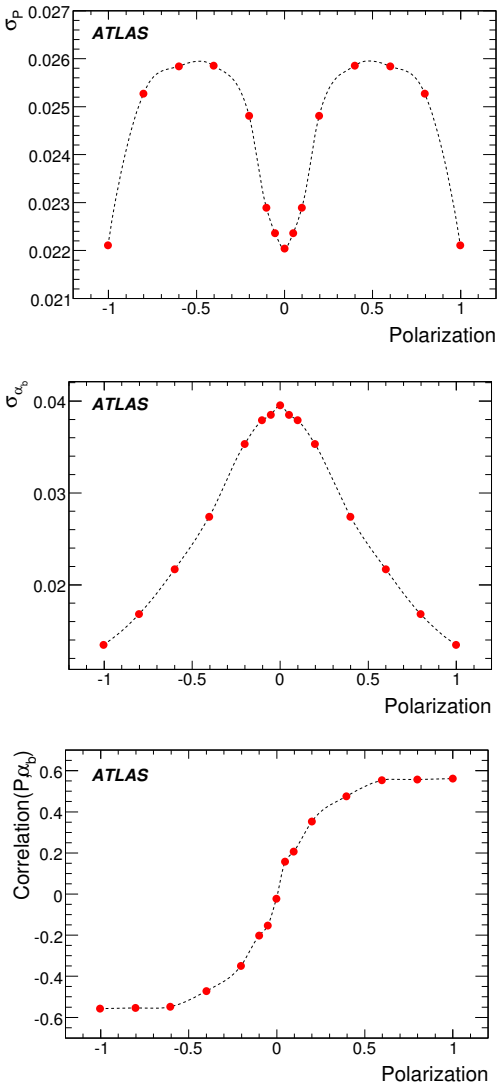

Figure 17: Expected statistical uncertainty on polarization (top) and on α_{Λ_b} (center) as a function of the polarization P. Bottom plot shows the expected correlation between α_{Λ_b} and the polarization P. All plots show results from the fast Monte Carlo study, obtained for the expected number of Λ_b events in data sample of 30 fb^{-1}.

regarded as a signal of an unexplained effect, either from the domain of existing physics, or of new physics altogether.

We further note that the development of Λ_b polarimetry as a tool for studying spin effects at the LHC could be important. For example, members for the SUSY community are quite interested in knowing what fraction of the b quark polarization ends up in the polarization of a Λ_b, since this could provide a way to test if b quark SUSY partners have the correct handedness. Only a few hundred Λ_b decays would be required to, for example, determine if its polarization were 100% or -100%. Challenges clearly exist, however, in determining the polarization transfer fraction, which requires a source of b's such as from $Z \to b\bar{b}$, and in dealing with the fact that only 10^{-5} of b's generate decay into the Λ_b channel we have described here. Our work on this

topic will continue.

Other related studies that should continue include mechanisms for comparing the α_{Λ_b} parameters from Λ_b and its antiparticle as a test of CP. We will accumulate data on both. If CP is conserved, the two parameters should be equal in magnitude but opposite in sign. While the precision of this test will not be high, and while models predict that any CP violation would be small in this sector, nevertheless, such a test would be unique in this domain and should be made.

Finally, as noted in Section 1, the lifetime of the Λ_b remains a topic of significant interest. Such a measurement will be a natural by-product of our efforts to extract the Λ_b spin parameters.

References

[1] C. Albajar *et al.*, Phys. Lett. B **243** (1991) 540.

[2] F. Gabbiani *et al.*, Phys. Rev. D **68** (2003) 114006.

[3] I. Dunietz, Z. Phys. C **56** (1992) 129.

[4] C. Q. Geng *et al.*, Phys. Rev. D **65** (2002) 091502.

[5] C. A. Nelson, Eur. Phys. J. C **19** (2001) 323.

[6] A. K. Giri *et al.*, Phys. Rev. D **65** (2002) 073029.

[7] D. J. Lange, Nucl. Inst. Meth. **A462** (2001) 152.
http::/www.slac.stanford.edu/∼lange/EvtGen/

[8] J. Szwed, Phys. Lett. B **105** (1981) 403.

[9] C. Chou *et al.*, Phys. Rev. D **65** (2002) 074030.

[10] W. G. D. Dharmaratna and G. R. Goldstein, Phys. Rev. D **53** (1996) 1073.

[11] W. G. D. Dharmaratna and G. R. Goldstein, Phys. Rev. D **41** (1990) 1731.

[12] K. Heller, Proceedings of the 9th International Symposium on High Energy Spin Physics, Bonn, Germany, p. 97, Springer-Verlag (1990).

[13] H. A. Neal and E. De La Cruz Burelo, AIP Conf. Proc. **915** (2007) 449 .

[14] Chung-Hsien Chou *et al.*, Phys. Rev. D **65** (2002) 074030; J. C. Collins, Phys. Rev. D **58** (1998) 094002; Chung-Hsien Chou, Int. J. Mod. Phys. A **18** (2003) 1429.

[15] J. Hrivnac *et al.*, J. Phys. G: Nucl. Part. Phys **21** (1995) 629.

[16] J. G. Korner and M. Kramer, Z. Phys. C **55** (1992) 659.

[17] P. Bialas *et al.*, Z. Phys. C **57** (1993) 115.

[18] R. Lednicky, Jad. Fiz. 43 (1986) 1275.

[19] T. Sjostrand *et al.*, Comp. Phys. Comm. **135** (2001) 238, eprint hep-ph/0108264.

[20] W. M. Yao *et al.*, J. Phys. G: Nucl. Part. Phys. **33** (2006) 1-1232.

[21] ATLAS-TDR-017; CERN-LHCC-2005-022.

[22] ATLAS TDR, CERNLHC99-15, Vol. II (1999) 614.

[23] A. C. Davison *et al.*, Bootstrap methods and their application, Cambridge Univ. Press (1997).

[24] H. Y. Cheng and B. Tseng, Phys. Rev. D **53** (1996) 1457.